CHEMISTRY
A EUROPEAN JOURNAL

DOI: 10.1002/chem.201101894

Efficient Preparation and Biological Evaluation of a Novel Multivalency Bifunctional Chelator for ^{64}Cu Radiopharmaceuticals

Shuanglong Liu, Zibo Li, Li-Peng Yap, Chiun-Wei Huang, Ryan Park, and Peter S. Conti*[a]

Positron emission tomography (PET) is a powerful imaging technique that provides in vivo information on the distribution of radiolabeled biomolecules. For example, 2-deoxy-2-^{18}F-fluoro-D-glucose (^{18}F-FDG) has successfully made PET a routine clinical practice in cancer diagnose, patient stratification, and monitoring the treatment of cancer patients.[1] The advancement of PET depends on the development of new radiotracers that will complement ^{18}F-FDG. Although PET nuclides ^{11}C ($t_{1/2}=20.4$ min) and ^{18}F ($t_{1/2}=109.7$ min) have been widely used for the development of PET imaging probes, their short half-lives set a strong limitation for evaluating bioactive ligands with long in vivo circulation time. ^{64}Cu ($t_{1/2}=12.7$ h) decays by β^+ (20%) and β^- emission (37%), as well as electron capture (43%), making it well suited for radiolabeling proteins, antibodies and peptides, both for PET imaging (β^+) and therapy (β^+ and β^-).[2] The low β^+ energy also promises a good resolution of down to 1 mm in PET images and guarantees minimal radiation doses to the patients during imaging scans.[3]

Because direct addition of ^{64}Cu into a targeting ligand (such as peptides and antibodies) is not practical, significant efforts have been devoted to the development of bifunctional chelators (BFCs) for ^{64}Cu. Currently, 1,4,7,10-tetra-azacyclododecane-*N*,*N*′,*N*″,*N*‴-tetraacetic acid (DOTA) is one of the most widely used chelators for ^{64}Cu labeling. However, its moderate in vivo stability would increase the non-targeted organ radiation dosage and lower the tumor-to-nontumor contrast.[4,5] ^{64}Cu-labeled radiopharmaceuticals with improved stability have been reported including 1,4,7-triazacyclononane-1,4,7-triacetic acid (NOTA) derivatives,[6–7] cross-bridged 1,4,8,11-tetraazacyclotetradecane-1,4,8,11-tetraacetic acid (CB-TETA),[5,8] and 1,4,8,11-tetraazabicyclo-[6.6.2]hexadecane (CB-TE2A) derivatives.[9–11] For these BFCs, relatively harsh conditions such as elevated temperature were generally required for ^{64}Cu chelation. Recently, a new class of BFCs has been synthesized based on the cage-like hexaazamacrobicyclic sarcophagine (denoted as "Sar", compound **2** in Scheme 1). The resulting ^{64}Cu complexes demonstrated great in vivo stability and efficient radiolabeling efficiency under mild conditions.[12–16] By modifying one of the inert primary amines of sarcophagine, a carboxyl-functionalized Sar (AmBaSar, Scheme 1) has been successfully developed in our laboratory.[12–14] As sarcophagine has two relatively inert primary amine groups on either end of its cage, we embarked on a project to develop novel Sar cage derivatives with multifunctional groups introduced to both ends. In the last decade, numerous studies have demonstrated that the multimer of a bio-active ligand in one single scaffold can improve both the cell-specific targeting efficacy and the tumor-targeting efficiency by several orders of magnitude.[17] In our first chelator design, we intended to introduce two pendant carboxyl groups at either end of the Sar cage (named BaBaSar), which could be further conjugated to multiple targeting ligands through biologically stable amide bonds. In order to prove the advantage of the multifunctional Sar chelators, we chose the *c*(RGDyK) peptide (denoted as RGD), a well-known ligand-targeting integrin $\alpha_v\beta_3$, for the construction of a divalent PET imaging probe.

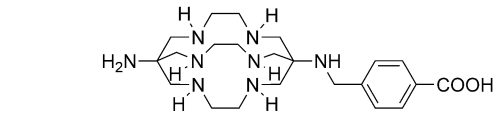

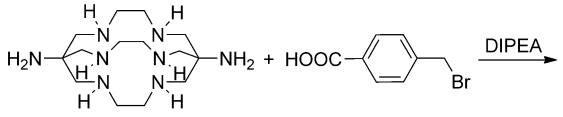

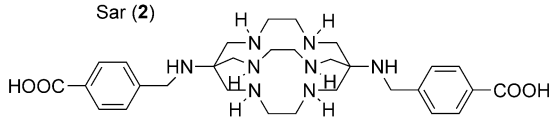

Scheme 1. Structure of AmBaSar and the synthetic scheme for BaBaSar. DIPEA = *N*,*N*-diisopropylethylamine.

[a] S. Liu,[+] Z. Li,[+] L.-P. Yap, C.-W. Huang, R. Park, Prof. P. S. Conti
Molecular Imaging Center, Department of Radiology
Keck School of Medicine, University of Southern California
1510 San Pablo Street, Room #350, Los Angeles, CA 90033 (USA)
Fax: (+1) 323-442-3253
E-mail: pconti@usc.edu

[+] These authors contributed equally to this work.

Supporting information for this article is available on the WWW under http://dx.doi.org/10.1002/chem.201101894.

We first improved the functionalization approach of the Sar cage. Previously, the benzoic acid moiety was introduced to the Sar cage through a four-step procedure (condensation, reduction, demetalation, and deprotection), which also included cation exchange purification and other complicated purification procedures.[12–14] The accumulated yield for AmBaSar was approximately 10% from compound **2**.[12] In our initial approach, we tried to obtain BaBaSar by simply increasing the stoichiometry of the methyl 4-formylbenzoate in order to introduce another benzoic acid moiety to AmBaSar. However, the synthesis became very difficult due to the multistep reactions and complicated crude compounds were obtained. After testing different approaches, we found that direct alkylation (S_N2) would be an efficient method for the synthesis of BaBaSar. As shown in Scheme 1, the protocol developed in our laboratory was followed for the synthesis of compound **2**,[12–14] which could then be directly alkylated with 4-bromomethylbenzoic acid to afford the product 4,4′-((3,6,10,13,16,19-hexaazabicyclo[6.6.6]ico-sane-1,8-diylbis(aza-nediyl))bis(methylene))dibenzoic acid (BaBaSar) in 36% yield. The monoalkylation product (AmBaSar) was also isolated in 30% yield.

After we obtained the bi-functionalized BaBaSar, its free carboxylic acid groups were activated with 1-ethyl-3-(3-dimethylaminopropyl)-carbodiimide (EDC)/*N*-hydroxysulfosuccinimide (SNHS) and then conjugated to *c*(RGDyK) in the presence of DIPEA. After HPLC purification, BaBaSar-RGD_2 was obtained in 78% yield (Scheme 2). The BaBaSar-RGD_2 was labeled with ^{64}Cu very efficiently in 0.1 M NH_4OAc buffer within 5 min at room temperature. The radiochemical yield (RCY) was as high as $(90.7\pm5.1)\%$ ($n=4$). The specific activity of ^{64}Cu–BaBaSar–RGD_2 was estimated to be 200–500 mCi μmol^{-1} (5.4–13.5 GBq μmol^{-1}). The in vitro stability of ^{64}Cu–BaBaSar–RGD_2 was evaluated after 1, 4, and 20 h incubation in 1×PBS buffer by radioHPLC (Figure S4 in the Supporting Information). Free ^{64}Cu was not detected by radioHPLC up to 20 h. These data are consistent with the previously published stability results.[12–16] The high stability could be due to the cross-bridged and cage-like configuration of the Sar structure. We also studied the metabolic stability of ^{64}Cu–BaBaSar–RGD_2 in blood, liver, kidneys, and tumor in nude mice bearing U87MG glioma xenografts at 1 h post injection. The intact probe was more than 95% in each examined organ by HPLC analysis (Figure S5 in the Supporting Information). On the contrary, the amount of intact tracer in blood, tumor, liver, and kidneys was only 38, 87, 34, and 74% for ^{64}Cu–DOTA–RGD at 1 h post injection, respectively.[13] These results further demonstrated the advantages of BaBaSar over DOTA in constructing ^{64}Cu radiopharmaceuticals.

The competitive U87MG cell-binding assay (IC_{50}) was used to determine the receptor $\alpha_v\beta_3$ binding affinity of BaBaSar–RGD_2, in which ^{125}I-echistatin was employed as a $\alpha_v\beta_3$-specific radioligand (Figure S6 in the Supporting Information). The IC_{50} of RGD dimer (RGD_2) was measured as a control. Both BaBaSar–RGD_2 and RGD_2 inhibited the binding of ^{125}I-echistatin to U87MG cells in a concentration-dependent manner. The IC_{50} values for BaBaSar–RGD_2, and RGD_2 were (6.0 ± 0.9) and (8.6 ± 1.2) nM, respectively ($n=3$). As expected, the BaBaSar–RGD_2 showed a strong binding affinity to U87MG cells and the introduction of the BaBaSar motif had minimal effect on the integrin binding affinity of the probe.

The in vivo tumor-targeting property of ^{64}Cu–BaBaSar–RGD_2 was evaluated by static microPET scans at 1, 4, and 20 h after injection of ^{64}Cu–BaBaSar–RGD_2 through the tail vain into 6–7 weeks old nude mice bearing U87MG tumors on the right shoulder. U87MG tumors were clearly visualized at all the time points examined (Figure 1). Region-of-interest (ROI) analysis on microPET images shows the tumor uptakes are (6.16 ± 0.88), (6.22 ± 1.42), and $(5.54\pm1.27)\%\,ID\,g^{-1}$ at 1, 4, and 20 h post injection, respectively (Figure 2A). The tumor/liver, tumor/kidneys, and tumor/muscle ratios reached (2.99 ± 0.46), (3.03 ± 1.19), and (20.27 ± 6.16) at 20 h post injection, respectively. As a consequence, the high tumor-to-nontumor ratio provided good contrast for PET imaging.

It is interesting to point out that ^{64}Cu–AmBaSar–RGD_2 (the two RGDs were introduced to the same side of the Sar cage, Scheme 2) gave significantly lower tumor uptakes values ($P<0.05$) which were (3.04 ± 0.25), (3.15 ± 0.21), and $(2.45\pm0.15)\%\,ID\,g^{-1}$ at 1, 4, and 20 h post injection, respectively.[18] The dramatic difference of these two otherwise similar structures might be due to the distance between the two RGD motifs. In the BaBa-

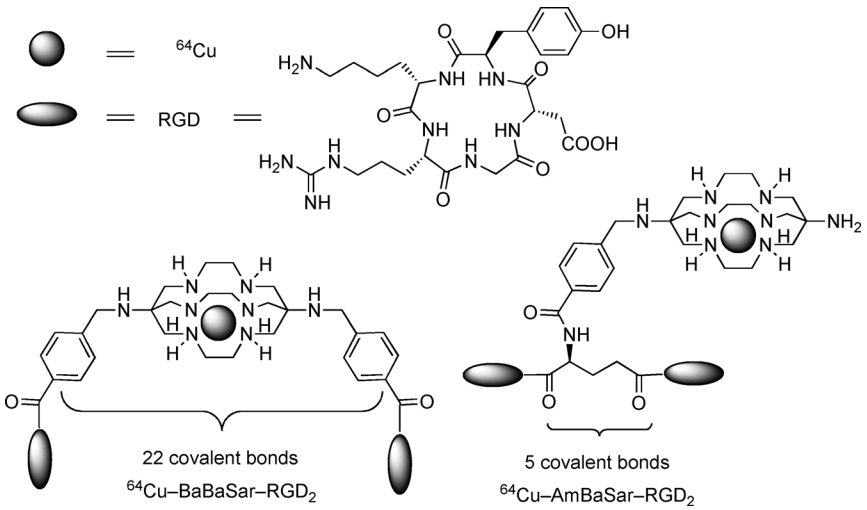

Scheme 2. Chemical structures of RGD and the corresponding cartoon structures of ^{64}Cu–BaBaSar–RGD_2 and ^{64}Cu–AmBaSar–RGD_2.

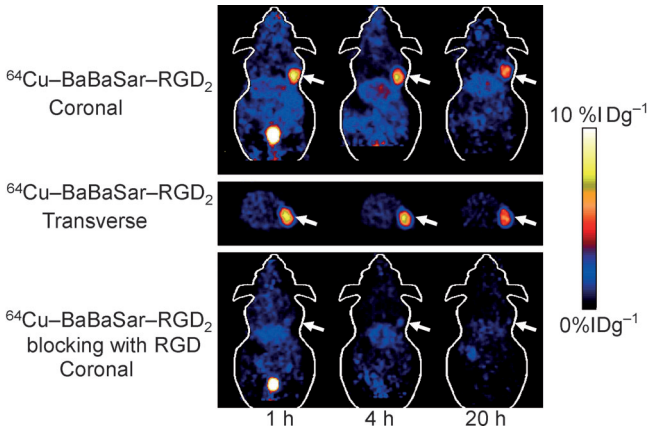

Figure 1. Decay-corrected whole-body microPET images of athymic female nude mice bearing U87MG tumor from a static scan at 1, 4, and 20 h after injection of ^{64}Cu–BaBaSar–RGD$_2$, with or without *c*(RGDyK) as blocking agent (10 mg kg^{-1} body weight). Tumors are indicated by arrows.

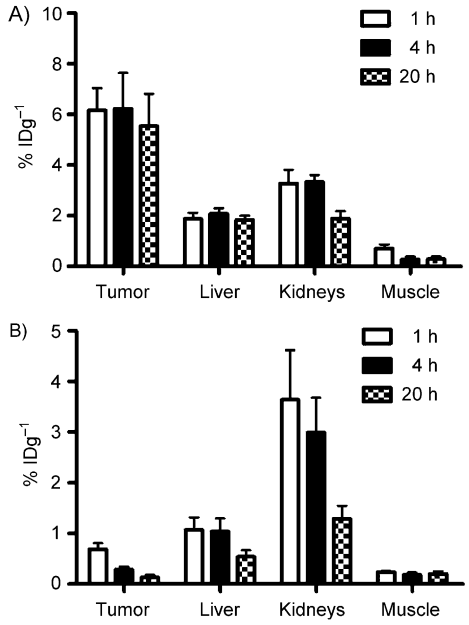

Figure 2. MicroPET quantification of tumors and major organs at 1, 4, and 20 h after injection of ^{64}Cu–BaBaSar–RGD$_2$. A) Without blocking agent. B) Co-injection with RGD as blocking agent (10 mg kg^{-1} body weight).

Sar–RGD$_2$, there are 22 covalent bonds between two RGDs, whereas there are only five covalent bonds between the two RGDs in the AmBaSar–RGD$_2$. The distance between the two cyclic RGD motifs in AmBaSar–RGD$_2$ is probably too short for simultaneously binding to two $\alpha_v\beta_3$ integrins (Scheme 2). Because the two RGD ligands in BaBaSar–RGD$_2$ have much longer distance and more flexibility, it may be more able to interact with two integrin receptors in the cell surface simultaneously. The much higher tumor targeting efficiency of ^{64}Cu–BaBaSar–RGD$_2$ also led to significantly higher tumor-to-nontumor ratios than those of ^{64}Cu–AmBaSar–RGD$_2$. For example, The tumor/liver ratio was only (0.86 ± 0.10) at 20 h post injection for ^{64}Cu–AmBaSar–RGD$_2$, compared with (2.99 ± 0.46) for ^{64}Cu–BaBaSar–RGD$_2$. This difference further demonstrated the superior properties of BaBaSar in constructing ^{64}Cu radiopharmaceuticals.

Blocking experiments were performed to confirm the integrin $\alpha_v\beta_3$ specificity of ^{64}Cu–BaBaSar–RGD$_2$. In the presence of a blocking dose of *c*(RGDyK), the U87MG tumor uptake was reduced to the background level and the uptake values were (0.69 ± 0.12), (0.29 ± 0.05), and (0.13 ± 0.05) % ID g^{-1} at 1, 4, and 20 h post injection, respectively. The uptake values in most of the normal organs (e.g., liver, kidneys, and muscle) were also lower than those without co-injection of *c*(RGDyK) (Figure 2B).

In conclusion, we have successfully demonstrated that the Sar cage could be efficiently functionalized through an alkylation reaction. The cage-like BaBaSar structure demonstrated favorable ^{64}Cu-labeling properties and the resulting ^{64}Cu–BaBaSar–RGD$_2$ showed great stability both in vitro and in vivo. The higher tumor uptake of ^{64}Cu–BaBaSar–RGD$_2$ compared to its ^{64}Cu–AmBaSar–RGD$_2$ analogue reflects the advantages of the BaBaSar scaffold. Herein, *c*-(RGDyK) was employed for proof of principle. In the future, two different biomarkers could be installed onto the two pedant arms of BaBaSar for constructing dual targeting probes. Furthermore, the two reactive sites of BaBaSar could be used to attach a targeting moiety on one side and an additional label (for secondary imaging modality) or therapeutic motif on the other side. We anticipate that this newly developed method will offer a novel way to construct multimodality imaging and therapeutic drugs.

Acknowledgements

This work was supported by the USC Department of Radiology, the Department of Energy (DE-SC0002353), the National Cancer Institute (P30A014089), and the USC Biomedical Imaging Science Initiative.

Keywords: bifunctional chelators · copper-64 · integrin $\alpha_v\beta_3$ · radiopharmaceuticals · RGD · sarcophagine

[1] M. Allen-Auerbach, W. A. Weber, *Oncologist* **2009**, *14*, 369–377.
[2] K. Chen, W. Cai, Z. B. Li, H. Wang, X. Chen, *Mol. Imaging Biol.* **2009**, *11*, 15–22.
[3] A. Chatziioannou, Y. C. Tai, N. Doshi, S. R. Cherry, *Phys. Med. Biol.* **2001**, *46*, 2899–2910.
[4] G. Niu, Z. Li, Q. Cao, X. Chen, *Eur. J. Nucl. Med. Mol. Imaging* **2009**, *36*, 1510–1519.
[5] C. A. Boswell, X. Sun, W. Niu, G. R. Weisman, E. H. Wong, A. L. Rheingold, C. J. Anderson, *J. Med. Chem.* **2004**, *47*, 1465–1474.
[6] H. S. Chong, S. Mhaske, M. Lin, S. Bhuniya, H. A. Song, M. W. Brechbiel, X. Sun, *Bioorg. Med. Chem. Lett.* **2007**, *17*, 6107–6110.
[7] A. F. Prasanphanich, P. K. Nanda, T. L. Rold, L. Ma, M. R. Lewis, J. C. Garrison, T. J. Hoffman, G. L. Sieckman, S. D. Figueroa, C. J. Smith, *Proc. Natl. Acad. Sci. USA* **2007**, *104*, 12462–12467.

[8] J. E. Sprague, Y. Peng, A. L. Fiamengo, K. S. Woodin, E. A. Southwick, G. R. Weisman, E. H. Wong, J. A. Golen, A. L. Rheingold, C. J. Anderson, *J. Med. Chem.* **2007**, *50*, 2527–2535.
[9] X. Sun, M. Wuest, G. R. Weisman, E. H. Wong, D. P. Reed, C. A. Boswell, R. Motekaitis, A. E. Martell, M. J. Welch, C. J. Anderson, *J. Med. Chem.* **2002**, *45*, 469–477.
[10] K. S. Woodin, K. J. Heroux, C. A. Boswell, E. H. Wong, G. R. Weisman, W. J. Niu, S. A. Tomellini, C. J. Anderson, L. N. Zakharov, A. L. Rheingold, *Eur. J. Inorg. Chem.* **2005**, 4829–4833.
[11] W. Liu, G. Hao, M. A. Long, T. Anthony, J. T. Hsieh, X. Sun, *Angew. Chem.* **2009**, *121*, 7482–7485; *Angew. Chem. Int. Ed.* **2009**, *48*, 7346–7349.
[12] H. Cai, J. Fissekis, P. S. Conti, *Dalton Trans.* **2009**, 5395–5400.
[13] H. Cai, Z. Li, C. W. Huang, R. Park, A. H. Shahinian, P. S. Conti, *Nucl. Med. Biol.* **2010**, *37*, 57–65.
[14] H. Cai, Z. Li, C. W. Huang, A. H. Shahinian, H. Wang, R. Park, P. S. Conti, *Bioconjugate Chem.* **2010**, *21*, 1417–1424.
[15] N. M. Di Bartolo, A. M. Sargeson, T. M. Donlevy, S. V. Smith, *J. Chem. Soc. Dalton* **2001**, 2303–2309.
[16] S. D. Voss, S. V. Smith, N. DiBartolo, L. J. McIntosh, E. M. Cyr, A. A. Bonab, J. L. Dearling, E. A. Carter, A. J. Fischman, S. T. Treves, S. D. Gillies, A. M. Sargeson, J. S. Huston, A. B. Packard, *Proc. Natl. Acad. Sci. USA* **2007**, *104*, 17489–17493.
[17] R. Haubner, H. J. Wester, *Curr. Pharm. Des.* **2004**, *10*, 1439–1455.
[18] H. Cai, Z. Li, C. W. Huang, R. Park, P. S. Conti, *Curr. Radiopharm.* **2011**, *4*, 68–74.

Received: June 21, 2011
Published online: August 4, 2011

